THE JOURNAL OF BIOLOGICAL CHEMISTRY VOL. 292, NO. 2, pp. 629–637, January 13, 2017

Activation of Latent Dihydroorotase from *Aquifex aeolicus* by Pressure*

Received for publication, May 25, 2016, and in revised form, October 14, 2016 Published, JBC Papers in Press, October 16, 2016, DOI 10.1074/jbc.M116.739862

Guy Hervé[‡1], Hedeel Guy Evans[§¶], Roshini Fernado[§], Chandni Patel[¶], Fatme Hachem[¶], and David R. Evans[¶2]

From the [‡]Laboratoire BIOSIPE, Sorbonne Universités, Institut de Biologie Paris Seine, CNRS, Université Pierre et Marie Curie, 75005 Paris, France, the [§]Department of Chemistry, Eastern Michigan University, Ypsilanti, Michigan 48197, and the [¶]Department of Biochemistry and Molecular Biology, Wayne State University School of Medicine, Detroit, Michigan 48201

Edited by Norma Allewell

Elevated hydrostatic pressure was used to probe conformational changes of *Aquifex aeolicus* dihydroorotase (DHO), which catalyzes the third step in *de novo* pyrimidine biosynthesis. The isolated protein, a 45-kDa monomer, lacks catalytic activity but becomes active upon formation of a dodecameric complex with aspartate transcarbamoylase (ATC). X-ray crystallographic studies of the isolated DHO and of the complex showed that association induces several major conformational changes in the DHO structure. In the isolated DHO, a flexible loop occludes the active site blocking the access of substrates. The loop is mostly disordered but is tethered to the active site region by several electrostatic and hydrogen bonds. This loop becomes ordered and is displaced from the active site upon formation of DHO-ATC complex. The application of pressure to the complex causes its time-dependent dissociation and the loss of both DHO and ATC activities. Pressure induced irreversible dissociation of the obligate ATC trimer, and as a consequence the DHO is also inactivated. However, moderate hydrostatic pressure applied to the isolated DHO subunit mimics the complex formation and reversibly activates the isolated subunit in the absence of ATC, suggesting that the loop has been displaced from the active site. This effect of pressure is explained by the negative volume change associated with the disruption of ionic interactions and exposure of ionized amino acids to the solvent (electrostriction). The interpretation that the loop is relocated by pressure was validated by site-directed mutagenesis and by inhibition by small peptides that mimic the loop residues.

Dihydroorotase (DHO)[3] is an amidohydrolase that catalyzes the reversible condensation of carbamoyl aspartate to form dihydroorotate in *de novo* pyrimidine biosynthesis in virtually all organisms (1, 2). Although the same reaction is catalyzed by all DHOs, the structure, oligomeric organization, and metal contentof this family of enzymes is diverse.

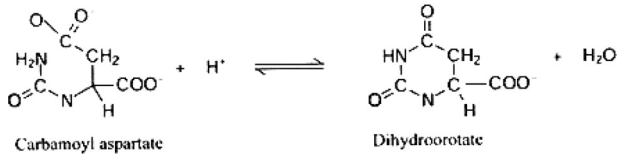

REACTION 1

A phylogenetic analysis has identified several distinct classes of dihydroorotase (3, 4). *Aquifex aeolicus* DHO forms a heterododecameric stoichiometric non-covalent complex with aspartate transcarbamoylase (ATC), the enzyme that catalyzes the formation of carbamoyl aspartate, the substrate for DHO.

Mammalian DHO is one of five major structural domains of the multifunctional protein CAD, which catalyzes the first three steps in the pyrimidine biosynthetic pathway (5). The polypeptide associates into a 1.45-MDa hexamer that exhibits glutamine-dependent carbamoyl phosphate synthetase, aspartate transcarbamoylase, and dihydroorotase activities. *A. aeolicus*, a prokaryotic extremophile of ancient lineage (6), catalyzes the same three steps in the pyrimidine pathway, but the homologous domains are separate polypeptide chains. We have cloned the genes encoding each of these five proteins and expressed them in *Escherichia coli* (7–10). Unlike the other individually cloned domains, all of which are fully functional, the *A. aeolicus* DHO, a 43-kDa monomer, lacked catalytic activity. However, the DHO subunit formed an active complex with *A. aeolicus* ATC consisting of six copies of each type of subunit that had both ATC and DHO activities (10).

The structure of the isolated *A. aeolicus* DHO subunit (11) is comprised of two domains, a distorted TIM barrel that resembles the structure of *E. coli* DHO (12), and a composite domain

* This work was supported in part by National Institute of Health Grants GM47399 and GM/CA60371 and National Science Foundation Grant MCB9810325. The authors declare that they have no conflicts of interest with the contents of this article. The content is solely the responsibility of the authors and does not necessarily represent the official views of the National Institutes of Health.

[1] To whom correspondence may be addressed: Laboratoire BIOSIPE, Sorbonne Universités, Institut de Biologie Paris Seine, Université Pierre et Marie Curie, 7 Quai Saint-Bernard, 75005 Paris, France. Tel.: 44-27-23-63; Fax: 44-27-23-61; E-mail: guy.herve@upmc.fr.

[2] To whom correspondence may be addressed: Dept. of Biochemistry and Molecular Biology, Wayne State University School of Medicine, 540 E. Canfield St, Detroit, MI 48201. Tel.: 313-577-1016; Fax: 313-577-2765; E-mail: ab2285@wayne.edu.

[3] The abbreviations used are: DHO, the *A. aeolicus* dihydroorotase subunit or activity; ATC, the trimeric *A. aeolicus* aspartate transcarbamoylase subunit or activity; DHO-ATC, the dodecameric complex consisting of six DHO and six ATC subunits.

present in many amidohydrolases (13–16). There are three flexible loops, designated A, B, and C that are disordered and invisible in the X-ray structure.

The isolated DHO subunit crystallized in two different space groups. These independent structures have nearly identical folds, except a water molecule was bound to the zinc in one X-ray structure (Protein Data Bank code 1xrf), whereas in the other structure (Protein Data Bank code 1xrt), Cys^{181} in loop A was ligated to the active site zinc, and a section of the loop completely occludes the active site, blocking access of the substrates. We then determined the X-ray structure of the *A. aeolicus* DHO-ATC complex (17), which showed that all of the disordered loops now had a well defined conformation and that an extensive movement of loop A had displaced it from the active site (Protein Data Bank code 3d6n). The experimental use of pressure can provide valuable and specific information about structure-function relationships in biomacromolecules, particularly proteins. This information relates to the volume changes (ΔV) associated with conformational changes, association-dissociation processes, and the variations of solvation that accompanies these phenomena. This approach is particularly useful in the study of enzyme catalytic and regulatory properties (18–21). In the present study, elevated hydrostatic pressure was employed to obtain information about its quaternary structural organization and interactions between the subunits in the *A. aeolicus* complex. However, during the course of this investigation, it was observed that moderate hydrostatic pressure could reactivate the isolated DHO in the absence of its partner, ATC. The hypothesis that elevated pressure mimics the conformational changes induced by the binding of ATC and displaces the loop occluding the DHO active site was verified by site-directed mutagenesis of residues that tether a segment of the loop in position (17) and with peptide inhibitors. The negative ΔV associated with the disruption of these interactions explains the reactivation of the isolated DHO by pressure. This interpretation is currently under further investigation by high pressure crystallography.

Results

Effect of Pressure on the DHO-ATC Dodecamer—As reported previously (10), the isolated DHO is inactive but is activated when associated with ATC. Elevated pressure typically, but not always, results in the dissociation of oligomers (19–21). To test the effect of pressure on the oligomeric structure and activities of the DHO-ATC complex, it was subjected to 800 bars for 1 h at 25 °C. Samples were taken at 10-min intervals, and both enzymatic activities were measured at atmospheric pressure and 75 °C (Fig. 1*A*). Both activities decreased with time of exposure to elevated pressure as the DHO-ATC complex dissociated.

As first observed for *E. coli* ATC (22–29), *A. aeolicus* ATC is a trimer, and each catalytic site is a composite, comprised of residues from adjacent subunits (9, 17). Consequently, dissociation of the trimer results in abolition of catalytic activity. Thus, the decrease in activity of ATC accompanying the dissociation of the trimer was anticipated, and because DHO is active only when associated with ATC, its activity might also be expected to decrease in parallel with the inactivation of ATC. However,

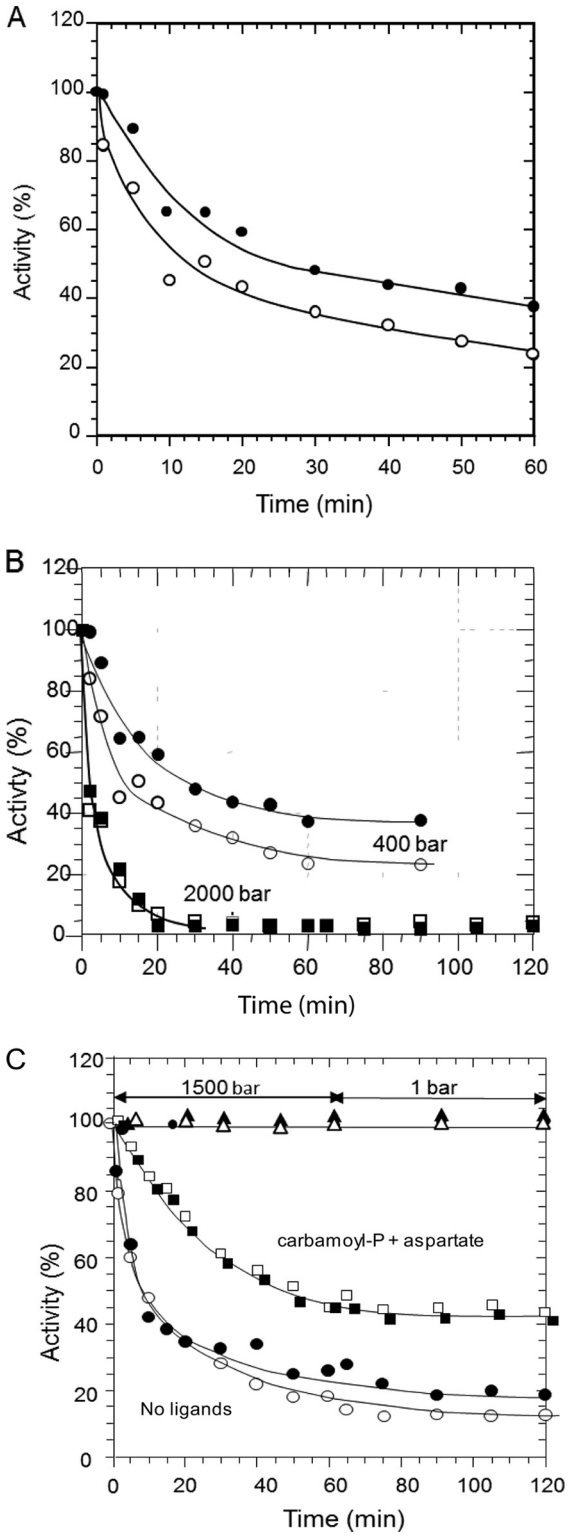

FIGURE 1. **Effect of pressure on the DHO-ATC complex.** *A*, the DHO-ATC complex was subjected to 800 bars for 1 h. Samples of 0.250 ml were taken at the indicated times, and the ATC (○) and DHO (●) activities were assayed as described under "Experimental Procedures." *B*, the same kind of experiment was performed at 400 bars (ATC ○ and DHO ●) and 2000 bars (ATC □ and DHO ■). After 1 h, the complex was returned for 30 min at atmospheric pressure, and a sample was taken. *C*, the DHO-ATC complex was incubated at 1500 bars in the presence (ATC □ and DHO ■) or absence (ATC ○ and DHO ●) of 1 mM carbamoyl phosphate and 5 mM of the aspartate analog, succinate for 1 h and then returned to 1 bar for an additional hour. As a control, the ATC (△) and DHO (▲) activities were measured in an identical sample kept at atmospheric pressure.

the DHO activity decreases more slowly than that of ATC, suggesting that there are other factors in play. The same experiment was performed at 400 and 2000 bars (Fig. 1*B*). The inactivation of both enzymes was slower at 400 bars and more rapid at 2000 bars as compared with the results obtained at the intermediate pressure. Again, DHO was inactivated more slowly at 400 bars, although this difference disappeared at 2000 bars where both activities were rapidly abolished at a comparable rate. No significant decrease of the activities was observed in the control samples kept at atmospheric pressure. After incubation under pressure, no recovery of the catalytic activities was observed after 30 min at atmospheric pressure. To verify that the pressure-induced inactivation of the DHO and ATC subunits is not reversible, the DHO-ATC complex was exposed to a pressure of 1500 bars for 1 h and then returned to atmospheric pressure. As expected, the rate of ATC inactivation was faster than that observed in Fig. 1*A*, and the difference in the rate of inactivation of ATC and DHO was less pronounced. When returned to atmospheric pressure, the activities remained virtually constant, indicating that the pressure-induced inactivation was irreversible.

The interpretation that dissociation of the ATC trimer was responsible for the loss of its catalytic activity was supported by subjecting the DHO-ATC complex to a pressure of 1500 bars in the presence of the ATC substrate, 1 mM carbamoyl phosphate, and 5 mM of the aspartate analog, succinate (Fig. 1*C*). Previous studies showed that these ligands protect the *E. coli* catalytic trimer from dissociation and inactivation by pressure.[4] Similarly, the inactivation of the *A. aeolicus* DHO-ATC complex is appreciably slower in the presence of the substrates (Fig. 1*C*). Moreover, the loss of DHO activity closely paralleled the inactivation of ATC. Again, no recovery was observed at atmospheric pressure.

The Effect of Pressure on the Isolated Subunits—The isolated DHO and ATC subunits were separately subjected to elevated hydrostatic pressure (1500 bars) for 1 h and then brought back to atmospheric pressure for an additional hour. Samples were taken periodically throughout the time course and assayed at 75 °C and atmospheric pressure (Fig. 2). Because DHO activity had only been observed in the DHO-ATC complex, a stoichiometric amount of ATC, which had not been subjected to pressure, was added to the assay after the sample had been removed from the chamber. Because adjacent subunits in the ATC trimer contribute active site residues, its dissociation results in abolition of catalytic activity. Previous studies have shown that elevated hydrostatic pressure dissociates the *E. coli* ATC catalytic subunit with a concomitant inactivation.[4] Similarly, the isolated *A. aeolicus* ATC subunit was rapidly inactivated at 1500 bars as the trimer dissociates (Fig. 2). There was no recovery of catalytic activity during the 1-h incubation after the sample was returned to atmospheric pressure, confirming that dissociation was irreversible, as observed previously for the *E. coli* catalytic subunit. In contrast, the monomeric DHO subunit appeared to be quite stable under these conditions; its activity, when subsequently assayed at 1 bar, was reduced by only 10% after 1 h at 1500 bars. This modest loss of activity was not reversed during the 1 h post-pressure incubation at 1 bar.

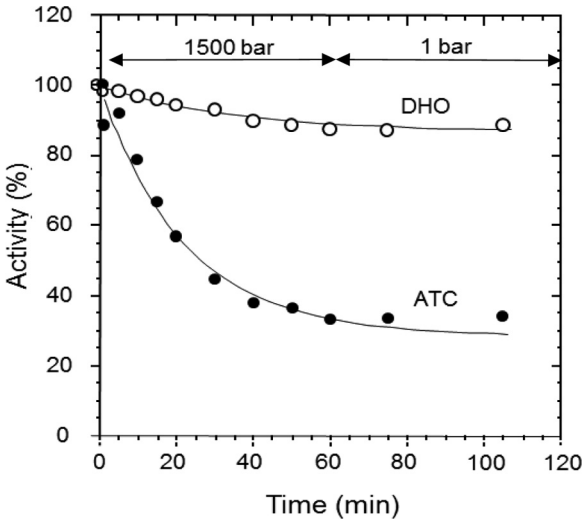

FIGURE 2. **Effect of pressure on the isolated ATC and DHO subunits.** ATC (●) and DHO (○) were incubated individually at 1500 bars for 1 h and then returned to atmospheric pressure for an additional hour. Samples of 0.250 ml were taken at the indicated times, and the activity was measured. For the DHO activity assays, ATC was added to the sample after removal from the high pressure instrument because at atmospheric pressure, the DHO is active only when the ATC is present.

Taken together, these results suggested that the inactivation of the two activities of the complex resulted from the pressure induced dissociation of ATC and that the integrity of the complex relies on the interactions between the ATC monomers in the catalytic trimer, a conclusion consistent with the dodecameric structural organization of the complex (17).

Influence of Pressure on the Activity of the Isolated DHO—In view of the slower pressure-induced decrease of DHO activity as compared with that of ATC, a direct influence of pressure on the activity of the isolated DHO subunit was suspected. In the experiments described thus far, the assays were carried out *after* the DHO-ATC complex had been subjected to elevated pressure and then returned to atmospheric pressure. In the following experiments, the substrate, dihydroorotate was present in the pressure chamber to assay the reaction under pressure. At atmospheric pressure, there is a very small residual DHO activity in the absence of ATC (Fig. 3) as reported previously (10). However, at 200 bars, the reaction proceeded at 57% of the rate observed at atmospheric pressure in the presence of the ATC subunit, indicating that there is a pressure induced activation of the DHO subunit. Control experiments verified that dihydroorotate is stable. No trace of carbamoyl aspartate could be detected during a 1-h incubation of dihydroorotate at 200 bars in the absence of the enzyme, whereas at 1 bar, little carbamoyl aspartate was produced by DHO.

Kinetics of the DHO Subunit under Pressure—Dihydroorotate saturation curves of the pressure activated DHO were conducted at increasing hydrostatic pressures (Fig. 4 and Table 1). The substrate was present in the pressure cell, and the reaction at each concentration was allowed to proceed for 10 min. The k_{cat} increases with increasing pressure to a maximum of 12.4 μmol/min/mg corresponding to a kcat of 10.1 s^{-1}, close to the

[4] G. Hervé and A. Else, manuscript in preparation.

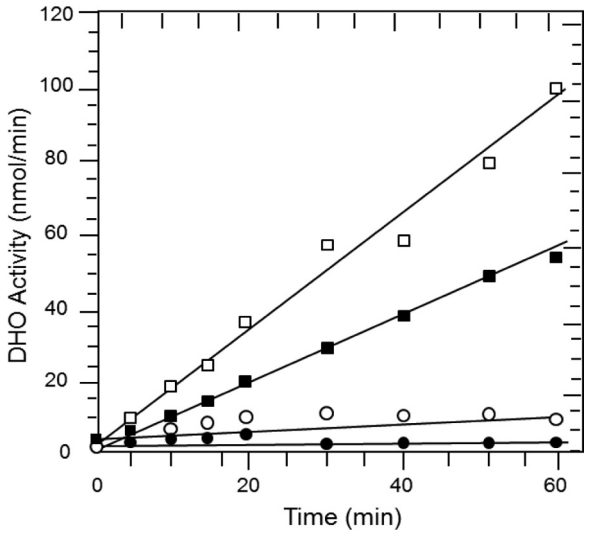

FIGURE 3. **Pressure-induced activation of the isolated DHO subunit.** The activity of the isolated DHO subunit was subjected to 200 bars in the presence of 8 mM dihydroorotate. Samples were taken at the indicated times, quenched, and then assayed by the colorimetric procedure ("Experimental Procedures") to determine the amount of product, carbamoyl aspartate (■) formed under pressure. The carbamoyl aspartate formed by the intact DHO-ATC complex was also determined at 1 bar (□). Control samples consisted of the isolated DHO subunit and dihydroorotate at 1 bar (○) and the formation of carbamoyl aspartate at 200 bars in the absence of the DHO subunit (●).

value obtained for the DHO-ATC complex. There was little pressure-dependent difference in the K_m values.

Reversibility of the Reactivation of DHO by Pressure—To determine whether the reactivation of DHO by pressure is a reversible process, the isolated enzyme was preincubated for 30 min at 200 bars and then returned to atmospheric pressure. Samples were taken at various times and tested for activity at 75 °C in the absence of ATC. No activity could be detected, indicating that the pressure-induced reactivation of DHO is fully reversible and that once returned to atmospheric pressure, DHO reverts to the inactive conformation.

Pressure Dependence of the Reactivation of the Isolated DHO and ΔV of Reactivation—The kinetics of the reaction catalyzed by the isolated DHO was measured as a function of pressure over one h incubations to determine the pressure-dependent variation of the rate constant (k). Half-maximal reactivation was observed at about 500 bars. The variation of $Ln(k)$ as a function of pressure (Fig. 5) is linear as expected on theoretical grounds, allowing calculation of the ΔV associated with reactivation. The slope of the plot gave a negative ΔV of -177 ± 4 ml/mol, a value consistent with the exposure to the solvent of a limited number of charged groups. This result suggested that the reactivation of the isolated DHO may result from the dissociation of loop A from the core of the enzyme similar to the displacement that occurs upon binding of the ATC subunit. This interpretation has been further investigated by site-directed mutagenesis and peptide inhibition experiments.

Mutation of Loop A Residues—Most of loop A is disordered. Only residues 179–187 are visible in the electron density map (Fig. 6). In addition to the interaction between Cys^{181} in loop A and the active site zinc ion (2.30 Å), two other residues anchor the loop in position (11). Asp^{179} forms a salt bond with Arg^{216} (3.15 Å), and Asp^{183} is hydrogen-bonded to Asn^{95} (2.78 Å) and

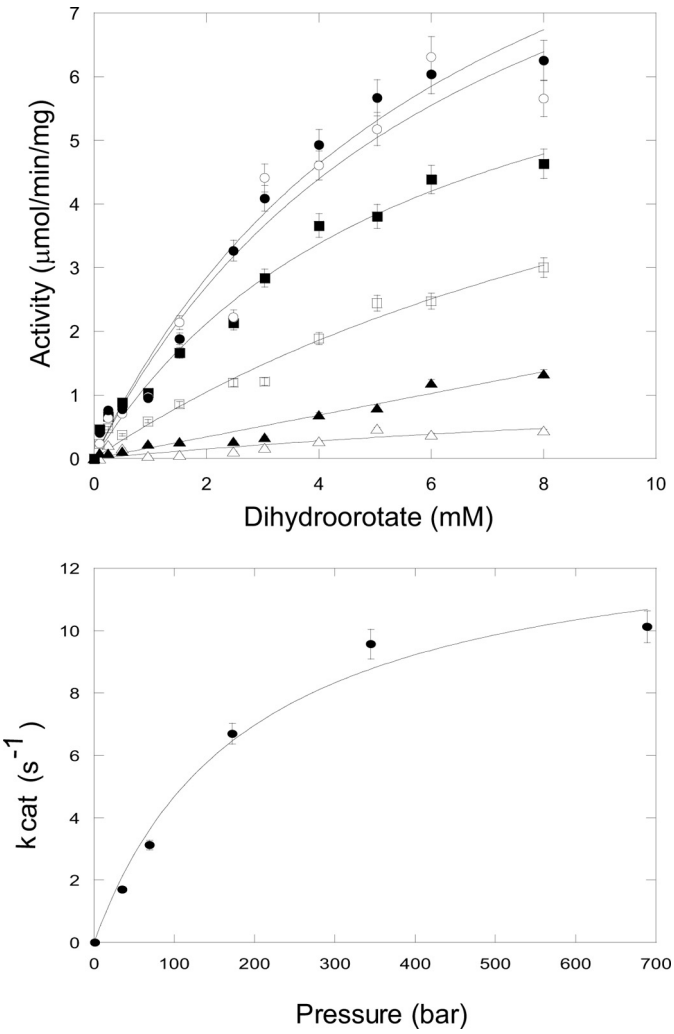

FIGURE 4. **Dihydroorotase kinetics of the isolated DHO subunit under pressure.** *Top panel*, dihydroorotate saturation curves. A reaction mixture contained 40 μg of the purified DHO subunit, and the indicated concentration of dihydroorotate was subjected to elevated pressures (*P* 1–700 bars) for 10 min at 25 °C. Carbamoyl aspartate formed was assayed as described under "Experimental Procedures." The data were fit to the Michaelis-Menten equation. *Bottom panel*, a plot of k_{cat}, calculated from the V_{max} values, against hydrostatic pressure.

TABLE 1
Kinetic parameter of pressure-activated DHO subunit

Pressure	K_m	V_{max}	k_{cat}
bar	*mM*	*μmol/min/mg*	s^{-1}
35	5.33	2.08	1.70
70	4.41	3.83	3.13
175	5.74 ± 1.29	8.20 ± 1.0	6.70
350	6.65 ± 2.77	11.7 ± 2.8	9.57
700	6.71 ± 1.72	12.4 ± 1.8	10.1

forms a salt link with His^{63} (2.33 Å). Each of these loop A residues was substituted with valine or glycine.

The effect of mutation of these residues on the DHO activity was assayed in the isolated DHO subunit as a function of the dihydroorotate concentration (Fig. 7 and Table 2). Each of these mutations significantly decreased the DHOase activity of wild type DHO-ATC. Consequently, the activation of the isolated DHO produced by the mutation was expressed relative that observed for the mutant DHO-ATC complex. The kinetic parameters for the isolated DHO mutant and in the DHO-ATC

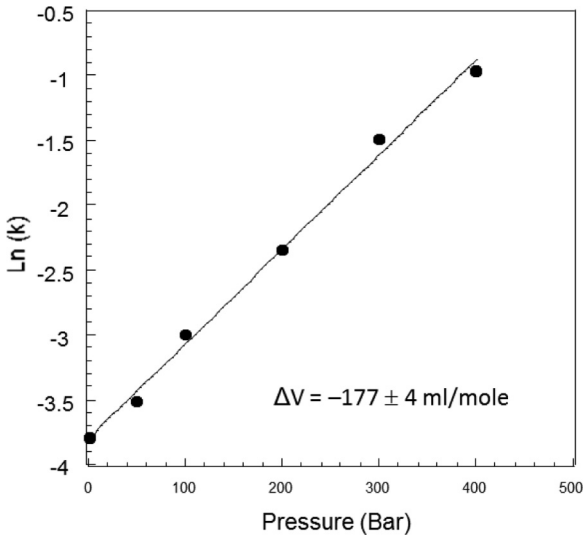

FIGURE 5. **Determination of the Δ*V* associated with the activation of the isolated DHO by pressure.** The initial velocity of the reaction catalyzed by the isolated DHO was measured as described under "Experimental Procedures" at various pressures from 1 to 400 bars. The *Ln* of the rate constants was plotted as a function of pressure. The Δ*V* of reactivation was calculated from the slope of the curve (slope = −Δ*V*/RT).

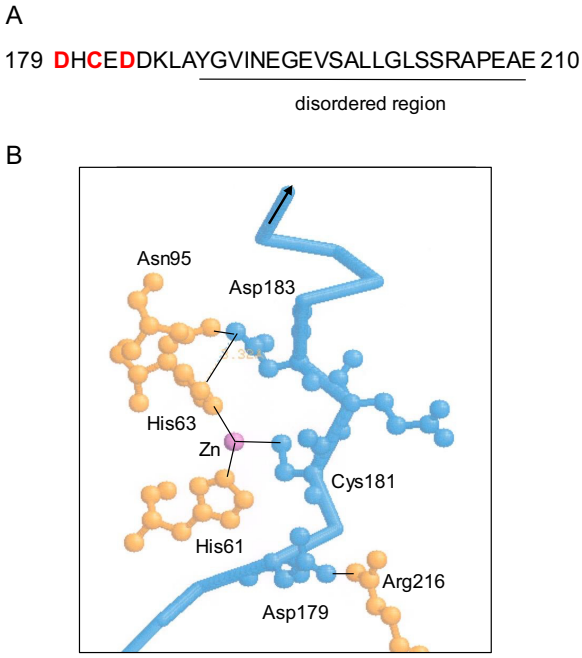

FIGURE 6. **Loop A interactions.** *A*, most of loop A is disordered and invisible in the electron density map of isolated DHO structures (residues 188–210), but residues 179–187 are visible and tethered by the interaction of loop A (*red*) with other regions of the isolated DHO subunit (11). *B*, three major interactions of loop A (*blue*) involved the zinc ligand, Cys^{181} (bond length, 2.6 Å), the salt bond between Asp^{179} in the loop A and Arg^{216} (3.15 Å), and a salt bond and a hydrogen bond between Asp^{183} in the loop and His^{63} and Asn^{95} (2.78 Å), respectively.

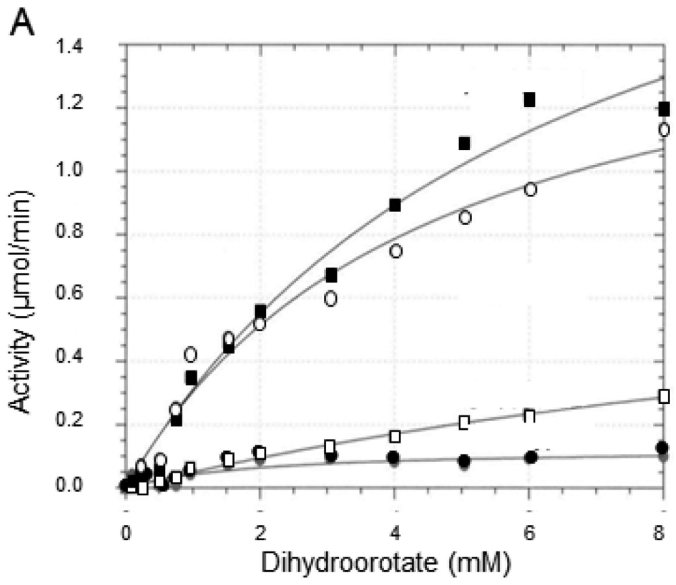

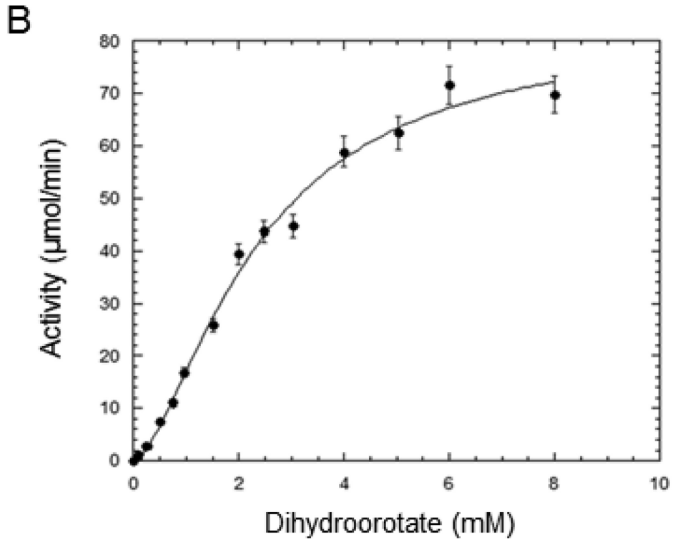

FIGURE 7. **Dihydroorotate saturation curve of the isolated DHO loop A mutants.** *A*, the DHO activity of the isolated DHO subunit was assayed as a function of dihydroorotate concentration as described under "Experimental Procedures" for the wild type (●), the D179V (○), the C181G (□), and D183V (■) mutants. *B*, dihydroorotate saturation curve of the wild type DHO-ATC complex (●).

complex where the mutant DHO subunit is maximally activated are given in Table 2. Replacement of Asp^{183} with valine activated the isolated subunit 68% compared with the maximum activity observed in the mutant complex. The replacement of Asp^{179} with valine resulted in a 33% activation, whereas the C181G mutant did not significantly activate the isolated DHO subunit.

Thus, the replacement of two of the residues known to dock loop A to the remainder of the protein results in activation of the latent DHO activity of the isolated subunit. These results are consistent with the hypothesis that pressure-induced activation results from a conformational change that moves loop A away from the active site, allowing substrate binding. The failure of the Cys^{181} mutant to restore catalytic activity suggests that this interaction does not significantly contribute to tethering loop A to the active site.

Effect of Peptides on the DHO Activity—The inhibition of the DHO activity by a series of small peptides that mimic the ordered region of loop A was assessed. If loop A is responsible for the inactivity of the isolated DHO subunit, then these peptides would also be expected to inhibit the active enzyme. The peptides ^{180}HCE^{182}, ^{179}DHCEDD^{185}, and ^{179}DHCEDDKLA^{187} were incubated at a concentration of 10 μM with the fully active

TABLE 2
Activation of loop A mutants by pressure

Mutant	DHO-ATC			DHO			DHO activation[a]
	V_{max}[b]	k_{cat}	K_m	V_{max}[b]	k_{cat}	K_m	
	μmol/min/mg	s^{-1}	*mM*	*μmol/min/mg*	s^{-1}	*mM*	%
Wild type	83.1 ± 5.4	62.3	2.38 ± 0.25	[c]	[c]	[c]	[c]
E179V	12.2 ± 0.7	9.2	0.24 ± 0.07	4.00 ± 0.46	3.0	6.2 ± 1.0	32.8
C181A	20.5 ± 3.2	15.5	3.89 ± 1.01	[c]	[c]	[c]	0
E183V	13.2 ± 1.0	9.7	0.47 ± 0.16	8.98 ± 2.04	6.7	24.0 ± 6.7	68.0

[a] The activation of the isolated DHO by the mutation was calculated as follows: percentage of activation = [V_{max} (isolated DHO)/V_{max} (DHO-ATC)] × 100.
[b] The assays were conducted at 74 °C, rather than 25 °C, the temperature at which the pressure experiments were conducted, so the V_{max} values are appreciably higher.
[c] Activity too low to obtain reliable values.

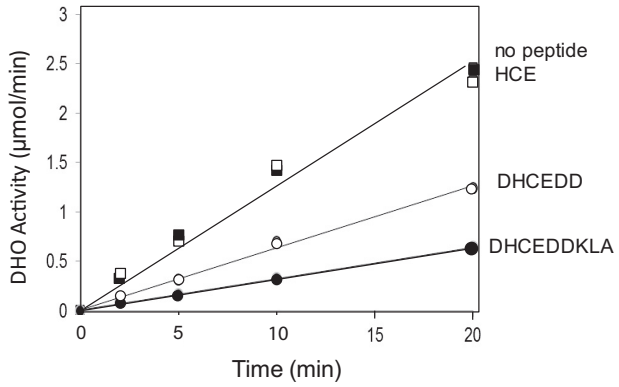

FIGURE 8. **Inhibition of DHO activity of the DHO-ATC complex by loop A peptides.** The DHO activity was assayed at 75 °C at a fixed concentration of dihydroorotate of 8 mM in the absence of peptides (■) and in the presence of the peptides ^{180}HCE^{192} (□), ^{179}DHCEDD^{184} (○), and ^{179}DHCEDDKLA^{1877} (●) at a concentration of 10 μM.

DHO-ATC complex for the indicated times (Fig. 8). ^{180}HCE^{182}, which includes the two residues flanking the cysteine bound to the zinc in the inactive enzyme, had no effect, whereas the other two larger peptides significantly inhibited the DHO activity of the complex: ^{179}DHCEDD^{185}, 50% inhibition; and ^{179}DHCEDDKLA^{187}, 76% inhibition.

Discussion

Elevated hydrostatic pressure was used to investigate the interactions and disassembly of the dodecameric DHO-ATC complex. When the complex was subjected to elevated pressure, in the absence of its substrates, both activities were rapidly lost at a rate that increased with increasing hydrostatic pressure. There was a parallel loss of DHO activity as expected because DHO is active only when associated with the intact ATC trimer (10). The rate of dissociation/inactivation was dependent on the magnitude of the pressure (Fig. 1). When the DHO-ATC complex was inactivated by subjecting it to elevated pressure for 1 h and then returned to atmospheric pressure for 1 h more, the activities were not recovered, indicating that the inactivation was irreversible.

Protection from pressure-induced inactivation of the *E. coli* trimeric ATC catalytic subunit by substrate analogs was previously observed.[4] The same result has been obtained here in the case of the DHO-ATC complex (Fig. 1*C*). The loss of ATC activity can be attributed to the dissociation of the trimer because the bound substrate analogs bridge the active site residues on adjacent subunits and stabilize the complex (24–29). The DHO activity was lost because it is dependent on association with a structurally intact ATC subunit. However, ATC and DHO activities were not simultaneously inactivated. Except at very high pressure (2000 bars), the inactivation of ATC significantly preceded the loss of DHO activity (Fig. 1). The interface between the DHO and the ATC monomers is quite extensive corresponding to 788 Å^2 (17). It is stabilized by nine H-bonds and seven salt bonds, so it is possible that the DHO subunit remains partially active via interactions with the fully or partially dissociated ATC subunit. However, it appeared that pressure had a positive influence on the activity of the isolated DHO.

The effect of pressure on isolated constituent subunits was also tested (Fig. 2). The activity of the ATC subunit decreased exponentially and irreversibly when incubated at 1500 bars (k = 0.018 min^{-1}) because of the dissociation of the obligatory trimeric structure. There was little effect on the activity of the DHO subunit when it was returned to atmospheric pressure and assayed in the presence of the ATC subunit, so pressure had little direct irreversible effect on the DHO structure and activity.

In the second series of experiments, the assays were conducted by introducing the substrate dihydroorotate into the pressure chamber rather than assaying the sample after it was returned to atmospheric pressure. These experiments were designed to directly access the influence of pressure on the catalytic activity of DHO. Unexpectedly, the isolated DHO became fully active in the absence of ATC. Up to this point, the DHO activity had only been observed in the complex, and virtually no activity has been observed in the presence of the same concentration of the substrate at ambient pressure.

We cannot rule out the possibility that reorganization of the other loops, which are disordered at ambient pressure, is also involved in catalysis. Two residues, Asn^{278} in loop B and Pro^{322} in loop C, are within hydrogen bonding distance of dihydroorotate in the DHO-ATC structure (17). These residues are not involved in the catalytic mechanism but may be significant in substrate binding. Once ordered (17), the remainder of loop is far from the catalytic site and appears to be primarily involved in establishing the interface between the DHO and ATC subunits. However, a more plausible explanation for the restoration of the catalytic activity under pressure is that loop A, which blocks access of the substrates to the active site, is displaced.

We can postulate that there is equilibrium between the inactive and active conformations of the isolated DHO subunit. At ambient pressure the equilibrium lies far toward the inactive conformation with loop A occluding the active site, but the direction of the equilibrium is reversed at elevated pressure.

DHO (loop in) *inactive* ⇌ DHO (loop out) *active*

REACTION 2

The interpretation that the two conformations of the protein are accessible at 1 bar is supported by the X-ray structures of the isolated DHO subunit; one structure (IIa) has the loop anchored and occludes the active site, whereas in the other (Ia) the loop is displaced with Cys^{181} relocated 8.36 Å from the catalytic zinc ion (11). We have no evidence that the postulated open conformation (Ia) is, in fact, catalytically active, although the X-ray structure indicates that although all of loop A residues (Asp^{179}–Asp^{210}) are disordered, the DHO active site residues are appropriately positioned as in the active site of the DHO-ATC complex (Fig. 8). The interatomic distances between key active site residues in the loop-out and the complex structures are within 0.5 Å in the two independent structures (Table 3). The salt bridge between Asp^{179} in loop A and Arg^{16} is disrupted in the open structure as it is in the partially active D179V mutant, an observation consistent with the idea that the open structure may be active.

There are four prominent interactions between bound dihydroorotate and the enzyme involving the residues Arg^{65}, Asn^{95}, Asn^{278}, and His^{309} (17) in DHO-ATC. With the exception of the Asn^{278}, which is part of the disordered loop B, these residues are appropriately placed in the DHO open structure (Fig. 9 and Table 3), albeit with slightly different orientations, suggesting that the loop-out structure of the subunit may be able to bind the substrate.

TABLE 3
Some interatomic distances between active site moieties

Residues or ion	Interatomic distance (Å)	
	DHO-ATC	DHO loop out
Arg^{65} (nh2)–Zn^{a}	7.48	7.31
Asn^{95} (od1)–Zn^{a}	5.93	5.83
Asp^{153} (od)^{a}–Zn^{a}	2.06	2.29
Asp^{305} (od)^{a}–Zn^{a}	3.40	3.31
His^{309} (ne2)–Zn^{a}	8.90	8.89
Arg^{65} (nh2)–His^{309} (ne2)	3.11	3.63
Asp^{153} (od)^{a}–His^{309} (ne2)	9.73	9.94
Asp^{305} (od)^{a}–His^{309} (ne2)	8.34	7.88
Asn^{95} (od1)-Arg^{65} (nh1)	4.19	4.01
Asp^{305} (od)^{a}–Asp^{153} (od)^{a}	4.96	5.44

^{a} Catalytic residue or ion.

A major effect of pressure on protein structure results from electrostriction (18, 19). Upon disruption of a salt bond, the water molecules surrounding the liberated charge are compressed as a result of the coulombic field of the charged group (electrostriction). This results in a decrease in the volume of the solution, a process that is favored by pressure.

Examination of the structure of the isolated DHO subunit (IIA) showed that loop A is tethered to the active site region by the zinc ligand, Cys^{181}, a salt link between Asp^{179} in loop A and Arg^{283} and a salt link and H-bond between Asp^{183} with His^{63} and Asn^{95}, respectively (Fig. 5). With the exception of Cys^{181}, mutation of these residues disrupts these interactions and partially restores the latent activity of the isolated DHO subunit.

The inhibition of DHO activity by a series of peptides with sequences corresponding to the segment of loop A near the active site was also assessed. The smallest peptide containing Cys^{181} (^{180}HCE^{182}) does not inhibit, consistent with the minimal effect of the C181G mutant on the activity of the isolated DHO subunit. The peptide ^{179}DHCEDD^{184}, containing tethering residues Asp^{179} and Asp^{183} identified in the loop-in DHO structure, is a good inhibitor, and a longer peptide from the same region (^{179}DHCEDDKLA^{187}) is more effective. This result suggests that the binding of loop A to the active site region is sufficient to inactivate DHO.

Except for pressure-induced dissociation of obligate oligomers, there are few examples in which moderate hydrostatic pressure alters enzyme activity. One notable exception is the pressure induced inactivation of α-chymotrypsin (32) resulting from the disruption of a salt link between Asp^{194} and Ile^{16}. Similarly, moderately elevated hydrostatic pressure induces the same open conformation in plasminogen as the binding of 6-aminohexanoate (33), a change that promotes the binding of streptokinase and plasminogen activation. Large changes in the rate of hydrolysis of β-lactoglobulin by thermolysin and pepsin were observed under elevated hydrostatic pressure (34).

The occlusion of the DHO active site by loop A prevents substrate binding and can largely account for the intrinsic inactivity of the isolated DHO subunit. This mechanism ensures that the DHO is active only when associated in a complex with

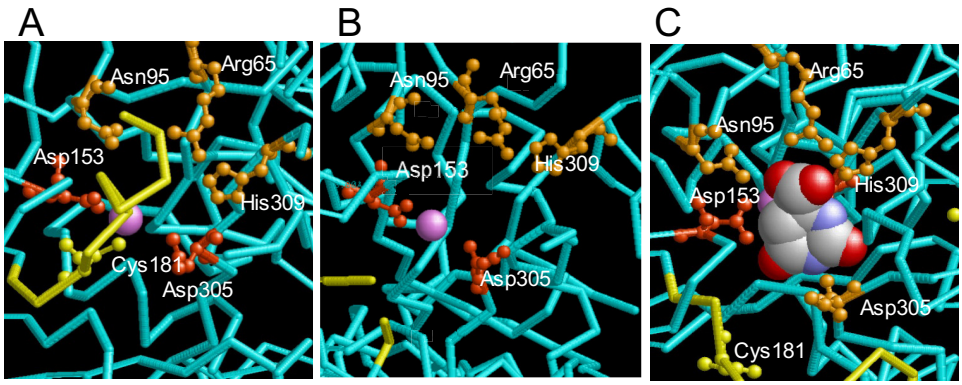

FIGURE 9. **Comparison of the active site structure of the loop-in, loop-out, and active DHO-ATC structures.** *A*, the isolated *A. aeolicus* DHO loop-in structure showing the occlusion of the active site by loop A (*yellow*). The catalytic residues Asp^{305} and Asp^{153} are shown in *red*, and the residues that bind dihydroorotate, Arg^{65}, Asn^{95}, and His^{309} are shown in *orange*. Asn^{278}, which also binds dihydroorotate, is invisible in this structure. *B*, the structure of the isolated *A. aeolicus* DHO loop-out structure showing loop A (*yellow*) displaced from the active site. *C*, structure of DHO active site in the DHO-ATC complex with bound dihydroorotate (*space filled*).

ATC. Moderate hydrostatic pressure appeared to induce an open conformation of the isolated DHO subunit. The architecture of the complex (17) is such that the reactions occur within a large internal central cavity, so the intermediate is transferred directly from its site of synthesis on the ATC subunit to the active site of the DHO subunit. At physiological pH, the equilibrium strongly favors the reverse reaction, the conversion of dihydroorotate to carbamoyl aspartate (35). If the isolated DHO subunit was catalytically active, any unassociated DHO would convert the dihydroorotate formed back to carbamoyl aspartate.

In summary, taken together, the kinetics of the isolated DHO under pressure, the site-directed mutations in loop A, and the inhibition of activity by the loop A peptides all indicate that pressure reactivates the isolated DHO by inducing an open conformation that moves loop A away from the entry to the catalytic site. This conclusion is presently being tested by crystallography under pressure.

Experimental Procedures

Materials—All chemicals were purchased from Sigma-Aldrich. *E. coli* strains DH5α and BL21 (DE3) were from Invitrogen.

Isolation of the DHO and ATC Subunits and Formation of the DHO-ATC Complex—The genes encoding *A. aeolicus* DHO (*pyrC*) and ATC (*pyrB*) subunits were previously cloned and separately expressed in *E. coli* (8, 9). The genes were identified in the *A. aeolicus* genome (6), amplified by PCR, and inserted into pRSETC (Invitrogen), an expression vector that incorporates a 3-kDa His tag on the amino end of the recombinant protein. The proteins were expressed individually in BL21 (DE3) and purified by Ni^{+2} affinity chromatography on a 1-ml Ni^{+2} Probond column (Invitrogen). The purified subunits were mixed in an equimolar ratio to reconstitute the dodecameric DHO-ATC complex (10, 17, 36). The complex was isolated by gel filtration chromatography on a Sephacryl S-300 column. The composition of the complex was analyzed by SDS-polyacrylamide gel electrophoresis (37) and ATC and DHO assays. Protein concentrations were determined by the Lowry method (38) using bovine serum albumin as a standard.

Enzyme Assays—The ATC activity was measured by monitoring the formation of carbamoyl aspartate using a colorimetric method previously described (39, 40). The reaction contained 2 mM aspartate, 5 mM carbamoyl phosphate, 1–11 μg of the purified enzyme, and 50 mM Tris-HCl, pH 8, in a total volume of 0.5 ml. The incubation time was 10 min at 25 °C or 1.5 min at 75 °C. The reactions were quenched by the addition of an equal volume of 5% acetic acid. The color was developed and quantitated as described previously (10).

DHO activity was measured (10) in the reverse direction, the formation of carbamoyl aspartate from dihydroorotate, because the equilibrium strongly favors dihydroorotate hydrolysis (35) at pH 8.3. The assay mixture consisted of 20–45 μg of DHO in 50 mM Tris acetate, pH 8.3. The reaction was initiated by the addition of dihydroorotate (8 mM or variable) and quenched by the addition of an equal volume of 5% acetic acid after 1.5 min (75 °C) or 10 min (25 °C). For reactions assayed at 75 °C, the assay mixture was equilibrated by preincubation at temperature for 1.5 min prior to initiation. Carbamoyl aspartate formed was determined by the same colorimetric method. The kinetic parameters were obtained by least squares analysis of the dihydroorotate saturation curves using the program KaleidaGraph 4.1 (Synergy Software).

High Pressure Experiments—The protein was subjected to elevated hydrostatic pressure in a reactor that allows removal of the samples of the reaction mixture via a pressure lock so that pressure inside the reaction chamber is not perturbed (30).

For assays at elevated hydrostatic pressure, the reaction mixture consisted of 2.10 ml of 0.5 M Tris HCl, pH 8, 0.40 ml of 2.0 mg/ml DHO (800 μg), and 15.1 ml of water. The reaction was initiated by the addition of 3.4 ml of 50 mM dihydroorotate. The reaction mixture, 19 ml was immediately transferred to the pressure chamber with the remaining 2 ml maintained at atmospheric pressure as a control. The chamber was pressurized, and 0.250-ml samples were taken at the indicated times and quenched into 0.250 ml of 5% acetic acid. The carbamoyl aspartate produced was measured as described above. For some experiments, a ISS (Champaign, Il) high pressure system with a 1.0 quartz cell was used.

Site-directed Mutagenesis—Site-directed mutagenesis was carried out by PCR as described previously (31) using *Pfu* Turbo polymerase from Stratagene (ThermoFisher) and the plasmid encoding the DHO subunit as a template. The residues in loop A suspected of anchoring the loop at the entry to the active site were replaced by valine or glycine using forward and reverse oligonucleotides from Invitrogen (ThermoFisher Scientific).

Author Contributions—G. H., H. G. E., and D. R. E. conducted the pressure studies, analyzed the results, and wrote the paper. R. F. conducted some of the pressure studies. R. F., F. H., and C. P. constructed the mutants and conducted the kinetic studies.

Acknowledgments—We thank the Department of Chemistry at Eastern Michigan University for purchasing the ISS (Champaign, IL) high pressure system and Prof. Thierry Foulon (Université Pierre et Marie Curie, Paris, France) for reading and improving this manuscript.

References

1. Jones, M. E. (1980) Pyrimidine nucleotide biosynthesis in animals: genes, enzymes, and regulation of UMP biosynthesis. *Annu. Rev. Biochem.* **49,** 253–279
2. Evans, D. R., and Guy, H. I. (2004) Mammalian pyrimidine biosynthesis: fresh insights into an ancient pathway. *J. Biol. Chem.* **279,** 33035–33038
3. Fields, C., Brichta, D., Shephardson, M., Farinha, M., and O'Donovan, G. (1999) Phlyogenetic analysis and classification of dihydroorotases: a complex history for a complex enzyme. *Paths Pyrimidines* **7,** 49–63
4. Grande-García, A., Lallous, N., Díaz-Tejada, C., and Ramón-Maiques, S. (2014) Structure, functional characterization, and evolution of the dihydroorotase domain of human CAD. *Structure* **22,** 185–198
5. Coleman, P. F., Suttle, D. P., and Stark, G. R. (1977) Purification from hamster cells of the multifunctional protein that initiates *de novo* synthesis of pyrimidine nucleotides. *J. Biol. Chem.* **252,** 6379–6385
6. Deckert, G., Warren, P. V., Gaasterland, T., Young, W. G., Lenox, A. L., Graham, D. E., Overbeek, R., Snead, M. A., Keller, M., Aujay, M., Huber, R., Feldman, R. A., Short, J. M., Olsen, G. J., and Swanson, R. V. (1998) The complete genome of the hyperthermophilic bacterium *Aquifex aeolicus*. *Nature* **392,** 353–358

7. Ahuja, A., Purcarea, C., Guy, H. I., and Evans, D. R. (2001) A novel carbamoyl-phosphate synthetase from *Aquifex aeolicus*. *J. Biol. Chem.* **276,** 45694–45703
8. Purcarea, C., Martin, P., Vickrey, J. F., Guy, H. I., Edwards, B. F., and Evans, D. R. (2002) Cloning, expression and preliminary X-ray analysis of the dihydroorotase from the hyperthermophilic eubacterium *Aquifex aeolicus*. *Acta Crystallogr. D Biol. Crystallogr.* **58,** 154–156
9. Purcarea, C., Ahuja, A., Lu, T., Kovari, L., Guy, H. I., and Evans, D. R. (2003) *Aquifex aeolicus* aspartate transcarbamoylase, an enzyme specialized for the efficient utilization of unstable carbamoyl phosphate at elevated temperature. *J. Biol. Chem.* **278,** 52924–52934
10. Ahuja, A., Purcarea, C., Ebert, R., Sadecki, S., Guy, H. I., and Evans, D. R. (2004) *Aquifex aeolicus* dihydroorotase: association with aspartate transcarbamoylase switches on catalytic activity. *J. Biol. Chem.* **279,** 53136–53144
11. Martin, P. D., Purcarea, C., Zhang, P., Vaishnav, A., Sadecki, S., Guy-Evans, H. I., Evans, D. R., and Edwards, B. F. (2005) The crystal structure of a novel, latent dihydroorotase from *Aquifex aeolicus* at 1.7A resolution. *J. Mol. Biol.* **348,** 535–547
12. Thoden, J. B., Phillips, G. N., Jr., Neal, T. M., Raushel, F. M., and Holden, H. M. (2001) Molecular structure of dihydroorotase: a paradigm for catalysis through the use of a binuclear metal center. *Biochemistry* **40,** 6989–6997
13. Ireton, G. C., McDermott, G., Black, M. E., and Stoddard, B. L. (2002) The structure of *Escherichia coli* cytosine deaminase. *J. Mol. Biol.* **315,** 687–697
14. Davies, M., Heikkilä, T., McConkey, G. A., Fishwick, C. W., Parsons, M. R., and Johnson, A. P. (2009) Structure-based design, synthesis, and characterization of inhibitors of human and *Plasmodium falciparum* dihydroorotate dehydrogenases (dagger). *J Med Chem.* **52,** 2683–2693
15. Xu, Z., Liu, Y., Yang, Y., Jiang, W., Arnold, E., and Ding, J. (2003) Crystal structure of D-hydantoinase from *Burkholderia pickettii* at a resolution of 2.7 Angstroms: insights into the molecular basis of enzyme thermostability. *J. Bacteriol.* **185,** 4038–4049
16. Vincent, F., Yates, D., Garman, E., Davies, G. J., and Brannigan, J. A. (2004) The three-dimensional structure of the *N*-acetylglucosamine-6-phosphate deacetylase, NagA, from *Bacillus subtilis*: a member of the urease superfamily. *J. Biol. Chem.* **279,** 2809–2816
17. Zhang, P., Martin, P. D., Purcarea, C., Vaishnav, A., Brunzelle, J. S., Fernando, R., Guy-Evans, H. I., Evans, D. R., and Edwards, B. F. (2009) Dihydroorotase from the hyperthermophile *Aquifex aeolicus* is activated by stoichiometric association with aspartate transcarbamoylase and forms a one-pot reactor for pyrimidine biosynthesis. *Biochemistry* **48,** 766–778
18. Heremans, K. (1982) High pressure effects on proteins and other biomolecules. *Annu. Rev. Biophys. Bioeng.* **11,** 1–21
19. Weber, G., and Drickamer, H. (1983) The effect of high pressure upon proteins and other biomolecules. *Q. Rev. Biophys.* **16,** 89–112
20. Mozhaev, V. V., Heremans, K., Frank, J., Masson, P., and Balny, C. (1996) High pressure effects on protein structure and function. *Proteins* **24,** 81–91
21. Hervé, G. (2010) High pressure in biology. In *Cell Mechanochemistry. Biological Systems and Factors Inducing Mechanical Stress, Such as Light, Pressure and Gravity* (van Loon, J., and Monici, M., eds) Transworld Research Network, Thiruvananthapuram, Kerala, India
22. Rosenbusch, J. P., and Weber, K. (1971) Subunit structure of aspartate transcarbamylase from *Escherichia coli*. *J. Biol. Chem.* **246,** 1644–1657
23. Wiley, D. C., and Lipscomb, W. N. (1968) Crystallographic determination of symmetry of aspartate transcarbamylase. *Nature* **218,** 1119–1121
24. Monaco, H. L., Crawford, J. L., and Lipscomb, W. N. (1978) Three-dimensional structures of aspartate carbamoyltransferase from *Escherichia coli* and of its complex with cytidine triphosphate. *Proc. Natl. Acad. Sci. U.S.A.* **75,** 5276–5280
25. Honzatko, R. B., Crawford, J. L., Monaco, H. L., Ladner, J. E., Ewards, B. F., Evans, D. R., Warren, S. G., Wiley, D. C., Ladner, R. C., and Lipscomb, W. N. (1982) Crystal and molecular structures of native and CTP-liganded aspartate carbamoyltransferase from *Escherichia coli*. *J. Mol. Biol.* **160,** 219–263
26. Krause, K. L., Volz, K. W., and Lipscomb, W. N. (1985) Structure at 2.9-A resolution of aspartate carbamoyltransferase complexed with the bisubstrate analogue *N*-(phosphonacetyl)-L-aspartate. *Proc. Natl. Acad. Sci. U.S.A.* **82,** 1643–1647
27. Krause, K. L., Volz, K. W., and Lipscomb, W. N. (1987) 2.5 A structure of aspartate carbamoyltransferase complexed with the bisubstrate analog *N*-(phosphonacetyl)-L-aspartate. *J. Mol. Biol.* **193,** 527–553
28. Kantrowitz, E. R., and Lipscomb, W. N. (1988) *Escherichia coli* aspartate transcarbamylase: the relation between structure and function. *Science* **241,** 669–674
29. Gouaux, J. E., and Lipscomb, W. N. (1988) Three-dimensional structure of carbamoyl phosphate and succinate bound to aspartate carbamoyltransferase. *Proc. Natl. Acad. Sci. U.S.A.* **85,** 4205–4208
30. Hoa, G. H., Hamel, G., Else, A., Weill, G., and Hervé, G. (1990) A reactor permitting injection and sampling for steady state studies of enzymatic reactions at high pressure: tests with aspartate transcarbamylase. *Anal. Biochem.* **187,** 258–261
31. Edwards, B. F., Fernando, R., Martin, P. D., Grimley, E., Cordes, M., Vaishnav, A., Brunzelle, J. S., Evans, H. G., and Evans, D. R. (2013) The mononuclear metal center of type-I dihydroorotase from *Aquifex aeolicus*. *BMC Biochem.* **14,** 36
32. Heremans, L., and Heremans, K. (1989) Raman spectroscopic study of the changes in secondary structure of chymotrypsin: effect of pH and pressure on the salt bridge. *Biochim. Biophys. Acta* **999,** 192–197
33. Kornblatt, J. A., Kornblatt, M. J., Clery, C., and Balny, C. (1999) The effects of hydrostatic pressure on the conformation of plasminogen. *Eur. J. Biochem.* **265,** 120–126
34. Dufour, G., Hervé, G., and Haertlé, T. (1995) Hydrolysis of β-lactoglobulin by thermolysin and pepsin under high hydrostatic pressure. *Biopolymers* **35,** 475–483
35. Christopherson, R. I., and Jones, M. E. (1980) The overall synthesis of L-5,6-dihydroorotate by multienzymatic protein pyr1–3 from hamster cells: kinetic studies, substrate channeling, and the effects of inhibitors. *J. Biol. Chem.* **255,** 11381–11395
36. Evans, H. G., Fernando, R., Vaishnav, A., Kotichukkala, M., Heyl, D., Hachem, F., Brunzelle, J. S., Edwards, B. F., and Evans, D. R. (2014) Intersubunit communication in the dihydroorotase-aspartate transcarbamoylase complex of *Aquifex aeolicus*. *Protein Sci.* **23,** 100–109
37. Laemmli, U. (1970) Cleavage of structural proteins during the assembly of the head of bacteriophage T4. *Nature* **227,** 680–685
38. Lowry, O. H., Rosenbrough, N. J., Farr, A. L., and Randall, R. J. (1951) Protein measurement with the folin phenol reagent. *J. Biol. Chem.* **193,** 265–275
39. Prescott, L. M., and Jones, M. E. (1969) Modified methods for the determination of carbamyl aspartate. *Anal. Biochem.* **32,** 408–419
40. Pastra-Landis, S. C., Foote, J., and Kantrowitz, E. R. (1981) An improved colorimetric assay for aspartate and ornithine transcarbamylases. *Anal. Biochem.* **118,** 358–363